PLOS ONE

RESEARCH ARTICLE

Targeting chronic cardiac remodeling with cardiac progenitor cells in a murine model of ischemia/reperfusion injury

Janine C. Deddens[1,2], Dries A. Feyen[1,3], Peter-Paul Zwetsloot[1], Maike A. Brans[1], Sailay Siddiqi[1], Linda W. van Laake[1,3], Pieter A. Doevendans[1,2,3], Joost P. Sluijter[1,2,3]*

1 Department of Cardiology, Experimental Cardiology laboratory, University Medical Center Utrecht, Utrecht, The Netherlands, **2** Netherlands Heart Institute (ICIN), Utrecht, The Netherlands, **3** Regenerative Medicine Center Utrecht, University Medical Center Utrecht, Utrecht, The Netherlands

* J.Sluijter@umcutrecht.nl

OPEN ACCESS

Citation: Deddens JC, Feyen DA, Zwetsloot P-P, Brans MA, Siddiqi S, van Laake LW, et al. (2017) Targeting chronic cardiac remodeling with cardiac progenitor cells in a murine model of ischemia/reperfusion injury. PLoS ONE 12(3): e0173657. https://doi.org/10.1371/journal.pone.0173657

Editor: Yiru Guo, University of Louisville, UNITED STATES

Received: November 26, 2016

Accepted: February 20, 2017

Published: March 20, 2017

Data Availability Statement: All relevant data are within the paper and its Supporting Information files.

Funding: We acknowledge the support from Innovation and the Netherlands CardioVascular Research Initiative (CVON): The Dutch Heart Foundation, Dutch Federation of University Medical Centers, the Netherlands Organization for Health Research and Development and the Royal Netherlands Academy of Science and the Alexandre Suerman program for MD/PhD students

Abstract

Background

Translational failure for cardiovascular disease is a substantial problem involving both high research costs and an ongoing lack of novel treatment modalities. Despite the progress already made, cell therapy for chronic heart failure in the clinical setting is still hampered by poor translation. We used a murine model of chronic ischemia/reperfusion injury to examine the effect of minimally invasive application of cardiac progenitor cells (CPC) in cardiac remodeling and to improve clinical translation.

Methods

28 days after the induction of I/R injury, mice were randomized to receive either CPC (0.5 million) or vehicle by echo-guided intra-myocardial injection. To determine retention, CPC were localized *in vivo* by bioluminescence imaging (BLI) two days after injection. Cardiac function was assessed by 3D echocardiography and speckle tracking analysis to quantify left ventricular geometry and regional myocardial deformation.

Results

BLI demonstrated successful injection of CPC (18/23), which were mainly located along the needle track in the anterior/septal wall. Although CPC treatment did not result in overall restoration of cardiac function, a relative preservation of the left ventricular end-diastolic volume was observed at 4 weeks follow-up compared to vehicle control (+5.3 ± 2.1 μl vs. +10.8 ± 1.5 μl). This difference was reflected in an increased strain rate (+16%) in CPC treated mice.

Conclusions

CPC transplantation can be adequately studied in chronic cardiac remodeling using this study set-up and by that provide a translatable murine model facilitating advances in

of the University Medical Center Utrecht, the Netherlands. Additionally, the ZonMW Translational Adult Stem Cell grant 1161002016.

Competing interests: The authors have declared that no competing interests exist.

Abbreviations: CVD, cardiovascular disease; CPC, cardiac progenitor cell; EF, ejection fraction; I/R, ischemia reperfusion; LAD, left coronary artery; LVEF, left ventricular ejection fraction; LVEDV, left ventricular end diastolic volume; LVESV, left ventricular end systolic volume; ECG, electrocardiogram; SR, strain rate; PSLAX, parasternal long axis; SAX, short axis; BA, basal-anterior; MA, mid-anterior; AA, apical-anterior; AP, apical-posterior; MP, mid-posterior; BP, basal-posterior; α-SMA, alpha smooth muscle actin.

research for new therapeutic approaches to ultimately improve therapy for chronic heart failure.

Introduction

Translational failure of novel therapies for cardiovascular disease (CVD) is a substantial problem involving both high research costs and an ongoing lack of novel treatment modalities reaching the bedside [1]. Although the overall mortality for CVD declined in the past decade, no improvement in survival after the diagnosis of heart failure is observed [2]. With a 5-year mortality rate of 50%, the high need for new treatment modalities is accentuated.

Cell based therapies have been implied as a novel approach for cardiac salvage and myocardial regeneration. Ever since the first clinical application of stem cells for acute ischemic heart disease more than a decade ago [3, 4], various studies demonstrated tentatively promising results regarding quality of life and cardiac parameters [5–7]. Despite the progress already made in a short period of time, application of cell therapy for chronic heart failure in a clinical setting is still hampered by poor translation [8]. Recent meta-analysis data shows that cell therapy in small animal models results in an improvement in ejection fraction (EF) of 11%, which is lowered to 5% when applied in large animal models and even further decreased to 3% in clinical studies [5, 9, 10].

The problem of clinical translation of stem cell therapy is complex and reasons for potential translational failure are diverse, including applied cell source, injury model and timing of therapy [11, 12]. One particular reason for the difficulty to translate functional outcomes from small to large animal models (and eventually to the clinic) is that cell therapy in small animal models is predominantly investigated in an acute myocardial injury setting [13]. Only a limited number of studies [14–17] tested stem cell therapy in small animals during chronic cardiac remodeling before switching to pre-clinical large animal research. To allow for correct (pre-) clinical translation, it is of great importance to study the basic mechanisms behind cell therapy in small animal models during this chronic remodeling phase.

In this regard, small animal models are extremely valuable in pre-clinical therapeutic research as they are easily accessible, relatively cheap and easy to manipulate genetically. However, it remains difficult to apply local therapeutics in murine chronic heart failure models due to the lack of accessibility to the heart after invasive MI surgery and the difficulty to use injection catheters in the small vascular anatomy of mice. Therefore, in this current study we provide an integrated model of chronic cardiac remodeling in mice, where we make use of a minimally invasive echocardiography-based local delivery strategy [18, 19]. As a proof of concept, we evaluate the use of human cardiac progenitor cells (CPC), an exciting class resident heart progenitor [20, 21], in our developed murine chronic ischemia/reperfusion (I/R) model.

Material and methods

(An expanded methods section is available in the S1 Appendix.)

Meta-regression analysis

We used the dataset of our meta-analysis [9] on placebo-controlled CPC studies in MI in small animals and complemented the data with a variable for CPC therapy timing. The primary outcome left ventricular ejection fraction (LVEF) was used for this analysis. We defined the acute

setting as CPC administration within 7 days after infarct, the sub-acute setting as between 7 and 28 days and a chronic MI model as CPC treatment after MI induction at 28 days or more. We used univariable meta-regression to test for a potential difference. Since this was a hypothesis-testing endeavor, we also included groups with less than 5 comparisons for our analyses of therapy timing.

CPC isolation, expansion and transduction

Human fetal heart tissue was obtained by individual permission using standard written informed consent procedures and prior approval of the ethics committee of the University Medical Center Utrecht, the Netherlands. This procedure is in accordance with the principles outlined in the Declaration of Helsinki for the use of human tissue or subjects. CPC were isolated by using Sca-1^+ conjugated magnetic beads as described previously [22]. Isolated CPC were able to differentiate into cardiomyocytes, endothelial cells and smooth muscle cells, confirming their stemness [23]. To facilitate identification *in vivo*, CPC were transduced with a lenti-viral construct, containing pLV-CMV-luc-GFP as described previously [24]. Cells were cultured in SP++ (M199, EGM2, FBS, P/S, NEAA) until 80% confluency and used for *in vivo* transplantation at passage 12-14.

Animals

All experiments were carried out in accordance with the Guide for the Care and Use of Laboratory Animals, with prior approval by the Animal Ethical Experimentation Committee, Utrecht University, the Netherlands. As CPC of human origin were studied, immune compromised mice (NOD-SCID mice, Harlan Laboratories) were used to prevent graft reaction.

Ischemia reperfusion model

Male NOD-SCID mice, aged 10-12 weeks, underwent left coronary artery (LAD) ligation as previously described [25, 26], followed by reperfusion after 60 minutes by releasing the ligature and removal of tubing. Reflow was confirmed by reversed discoloration of the heart.

Cell transplantation model

Twenty-eight days after induction of myocardial injury, animals were injected with either CPC, or vehicle (PBS) (Fig 1). To determine the extent of injury, mice underwent echocardiography (echo) followed by randomization in the different groups. Mice were positioned in an adjusted parasternal long axis view (PSLAX) for intramyocardial injection. CPC or vehicle were injected in the anterior wall via a transthoracic approach with echo guidance. A 27 Gy needle was used and 0.5 million cells were injected in two times 5 μl targeting the same 'borderzone' region.

Bioluminescent imaging (BLI)

To determine the amount of engrafted CPC, emitted photons by CPC-luc were detected two days after injection by the photon imager from Biospace Laboratory and analyzed by Photovison software as previously described [24]. Injections were considered successful based on a threshold of BLI signal 2 days after injection ($>$ 20.000 ph/s/cm^2/sr), established with previously performed titrations [24]. After primary outcome analyses, animals with a low retention ($<$ 20.000 ph/s/cm^2/sr) were used for additional analyses.

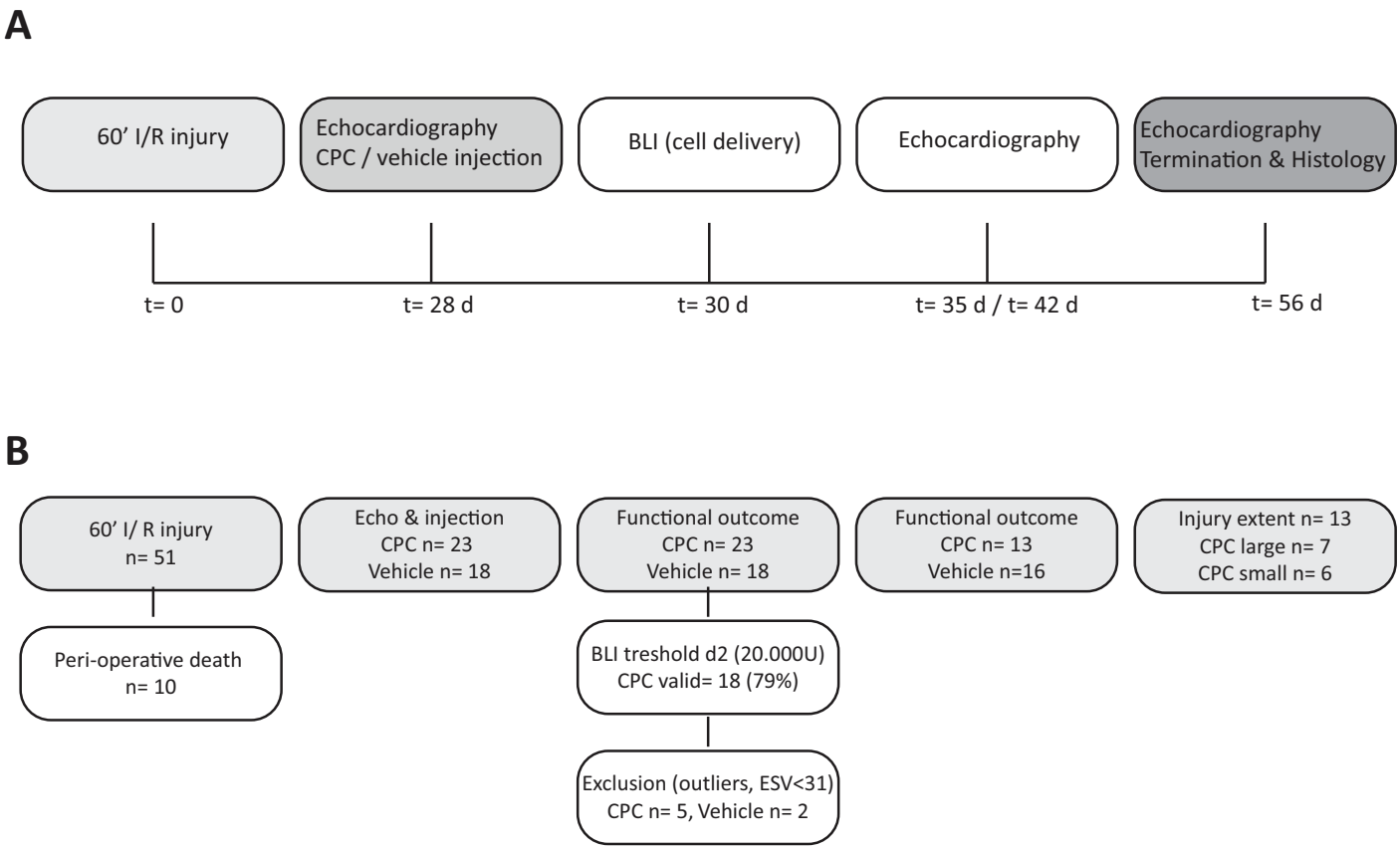

Fig 1. Study protocol. A) Timeline diagram of procedures and **(B)** flowchart of mouse experiment. Mice without significant cardiac damage (LVESV< 31), outliers or unsuccessful CPC injections (BLI signal after 2 days <20.000U) were excluded from primary analysis. For additional analysis, the CPC group was divided based on injury extent with the median LVEDV prior to cell treatment as cut-off point. 'CPC small' refers to animals with a LVEDV <median and 'CPC large' to animals with a LVEDV >median.

https://doi.org/10.1371/journal.pone.0173657.g001

3D motor echocardiography

Echo was performed at baseline, 28 days after I/R injury and at 7,14 and 28 days after treatment using a high resolution ultrasound system (Vevo 2100, VisualSonics) with a 18-38 MHz transducer (MS 400, VisualSonics). Echo acquisition and all analyses were performed by a blinded investigator. Left ventricular end-diastolic volume (LVEDV) and left ventricular end-systolic volume (LVESV) were used to calculate LVEF.

Pre-treatment echo measurements were analyzed and animals without significant cardiac damage, defined as an LVESV< 31 μl (= mean baseline value + 2x standard deviation) were excluded. Additionally, outliers were identified using the ROUT method (Q = 1%; [27]) and were excluded from further analyses. For additional analysis, the CPC group was divided based on injury extent with the median LVEDV prior to cell treatment as cut-off point.

Post measurement speckle tracking based analyses were performed to determine myocardial deformation parameters (VevoStrain, VisualSonics). Echo images acquired from the PSLAX were used to measure peak velocity (cm/s), strain (%) and strain rate (SR)(1/s) in the longitudinal and radial axis. For global measurements the average of all 6 myocardial segments (basal-anterior (BA), mid-anterior (MA), apical-anterior (AA), apical-posterior (AP), mid-posterior (MP) and basal-posterior (BP)) was taken. The infarct area was defined as the average of MA, AA and AP.

Histological analysis

At day 28 after intramyocardial injection with either CPC or vehicle, mice were terminated by exsanguination under general anesthesia and their hearts were excised. The hearts were dehydrated and fixed in a 15% sucrose 0.4% PFA solution after which they were embedded in O.C.T. compound (Tissue Tek) and stored at -80˚C. Serial transverse cryosections of 7 μm were cut, base to apex, for histological and immunohistological stainings. Imaging and analysis were performed by a blinded investigator.

Statistical analysis

Statistical analyses were carried out using GraphPad Prism 6.0 software (GraphPad Software, La Jolla, USA). Data is presented as mean ± SEM and were compared using the two-tailed Student's T-test. For analyses in time, the two-tailed paired Student's T-test was performed. $p < 0.05$ was considered statically significant.

Results

Meta-regression

To systematically explore the effect of CPC in chronic cardiac remodeling, we performed meta-regression for the timing of therapy in our dataset of placebo-controlled small animal CPC studies for MI. The dataset contained 95 comparisons, of which 5 comparisons were in the sub-acute phase (1-4 weeks) and only 2 administered their therapy in a chronic MI setting (> 4 weeks after MI induction). Meta-regression showed a large spread in effect on LVEF for the timing of therapy (S1 Fig, p = 0.258). The low number of studies and large spread in effect endorsed our *in vivo* study.

Cardiac engraftment and localization of CPC after echo guided intramyocardial injection

A total of 51 mice were used in this study of which 10 mice died periprocedural. All other 41 animals were included in this study and 23 mice were injected with CPC (Fig 1).

To determine retention of transplanted CPC in the chronic remodeling heart, cells were localized *in vivo* by BLI two days after echo-guided injection (Fig 2A). Furthermore, cells were traced *ex vivo* with an anti-human lamin A/C antibody to confirm their presence and human origin. BLI showed a detectable signal in the targeted region in all CPC injected mice. Seventy-eight percent (18/23) of the injections were considered successful based on our previously determined threshold of BLI signal 2 days after injection (> 20,000 ph/s/cm2/sr [24], Fig 2B). CPC remained in the tissue up to 28 days after injection and were mainly located along the needle track in the anterior and septal wall (Fig 2C–2E). Transplanted CPC demonstrated an intact nuclear pattern and did not show clear tissue integration.

I/R model in NOD-SCID mice

Pre-treatment echo measurements were analyzed and animals without significant cardiac damage, defined as an LVESV< 31 μl (= mean baseline value + 2x standard deviation) were excluded (n = 4). Additionally, 3 animals were defined as outliers using the ROUT method (Q = 1%; [27]) and were excluded. Representative echocardiographic images (three-dimensional reconstructions) of LVEDV and LVESV after I/R injury can be found in S2 Fig.

The geometry of the left ventricle was significantly altered upon MI, confirming successful induction of adverse cardiac remodeling. After 4 weeks, LVEDV (66.3 ± 1.5 μl to 78.5 ± 1.3μl)

and LVESV (26.5 ± 0.7 μl to 41.2 ± 1.6 μl) were significantly increased ($p < 0.001$). Cardiac performance was affected by these changes, represented in a decrease in LVEF (60.1% ± 0.8 to 48.0% ± 1.3, $p < 0.0001$). No differences in cardiac geometry or function were observed between both experimental groups before treatment (LVEDV p = 0.78, LVESV p = 0.69, LVEF p = 0.95; Fig 3A–3C).

Adverse cardiac remodeling is attenuated by CPC treatment

Treatment with CPC 28 days after I/R injury resulted in preservation of the LVEDV at 4 weeks follow-up (day 56 of experiment) compared to vehicle control (+5.3 ± 2.1 μl vs. +10.8 ± 1.5 μl,

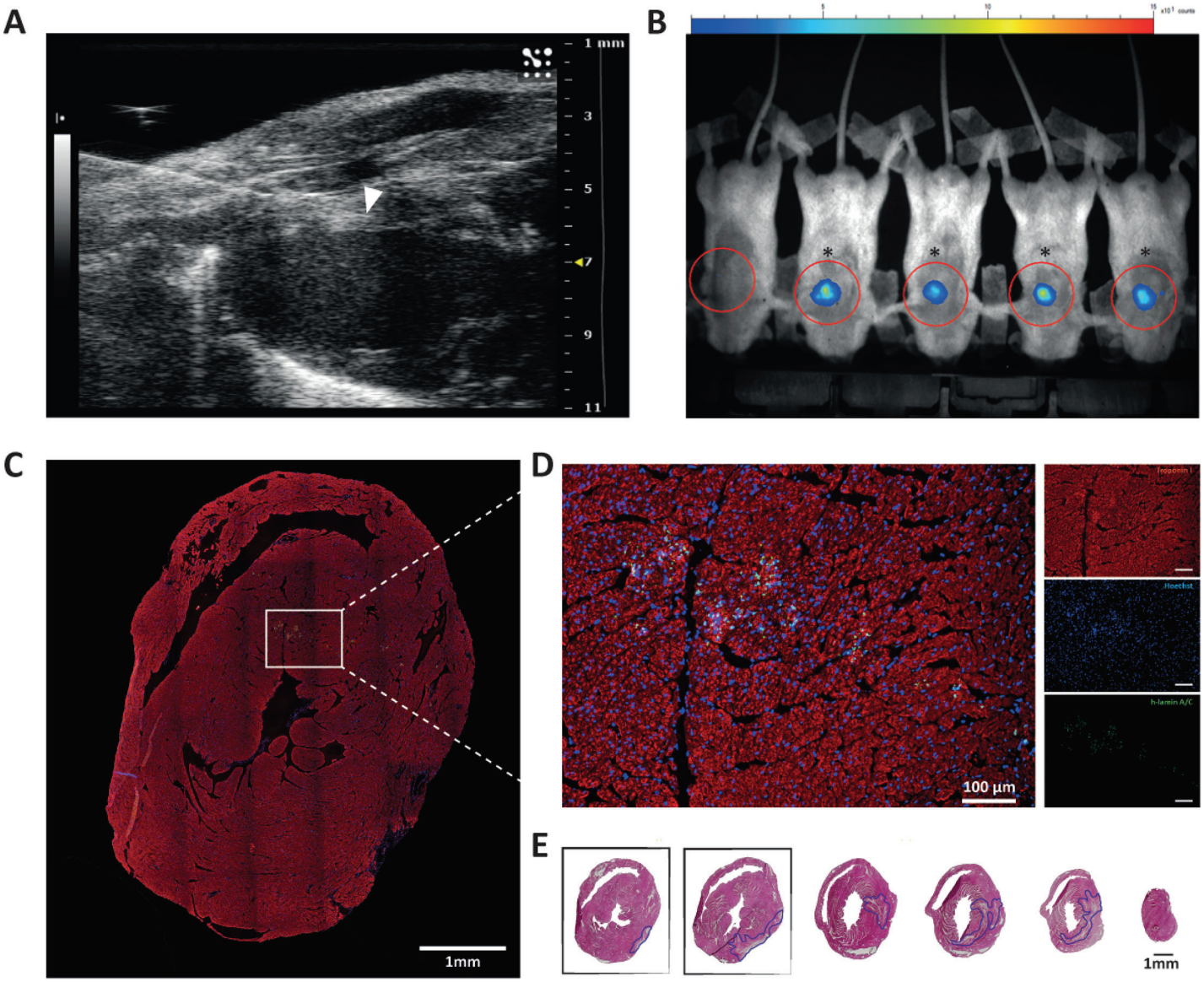

Fig 2. Echo-guided intramyocardial injection resulted in successful delivery of CPC. A) Representative B-mode image of intra-myocardial injection (29 Gy needle) at 4 weeks after the onset of I/R injury. The needle tip (marked by white arrowhead) is located in the anterior wall of the left ventricle. **B)** BLI images 2 days after intramyocardial injection with CPC demonstrated that 18/23 injections were successful (marked with *). **C-D**) CPC retained in the tissue up to 28 days after injection, as visualized by immunofluorescent staining for human lamin A/C (green), troponin I (red) and nuclei (blue). CPC were predominantly located along the needle track in the anterior and septal wall, at the level of the papillary muscles. (**E**) Squares mark H&E slides at the level of traced CPC. The left sided H&E slide corresponds to the CPC tracing slide in 'C and D'.

https://doi.org/10.1371/journal.pone.0173657.g002

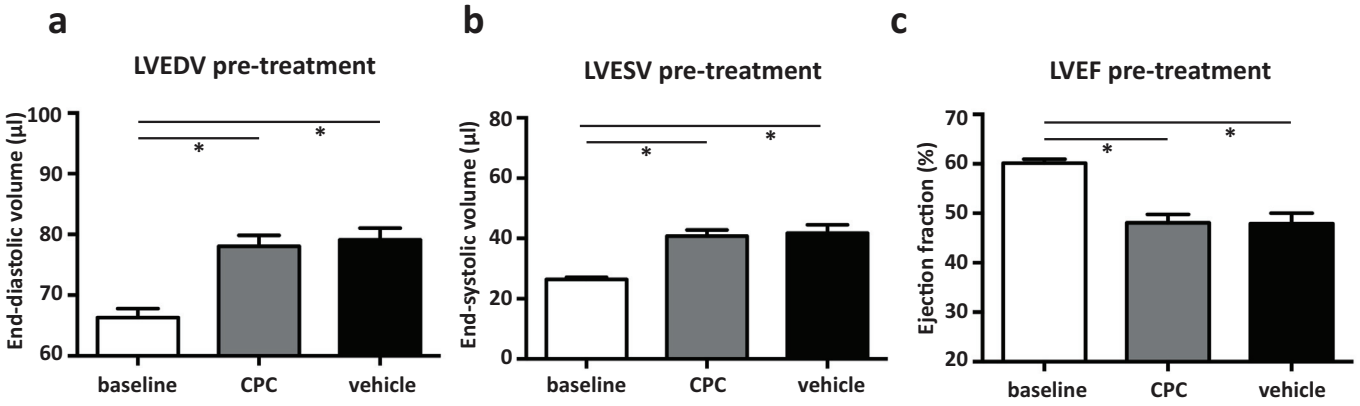

Fig 3. Functional measurements by echocardiography of day 28 (pre-treatment). Upon I/R injury the LVEDV (A) and LVESV (B) are increased, and the LVEF (C) is decreased with no differences between CPC treated or vehicle treated mice. CPC group: n = 19, Vehicle group; n = 16. * p< 0.001.

https://doi.org/10.1371/journal.pone.0173657.g003

p = 0.036; Fig 4A). This difference was even more pronounced in mice with more left ventricular remodeling (+4.4 ± 2.6ul vs. +12.3 ± 2.5 µl, p = 0.045) compared to mice with a smaller injury (+6.3 ± 3.7 µl vs. +9.3 ± 1.7 µl, p = 0.43) (S3 Fig). To define this difference in extent of injury, we used the median LVEDV prior to cell treatment as cut-off point. Although not significant, the differential effect of CPC treatment was already observed 14 days after treatment (+4.7 ± 2.5 µl vs. +8.2 ± 2.2 µl, p = 0.3). Interestingly, this attenuation was not observed in the CPC group with low retention signals based on BLI two days after injection compared to vehicle control (+12.4 ± 5.0 µl vs. +10.8 ± 1.5 µl, p = 0.69; S3 Fig). In contrast to the observed differences in LVEDV, LVESV was uniformly increased in both CPC and vehicle treated mice (+6.4 ± 1.8 µl vs. +4.6 ± 1.7 µl, p = 0.48) and appeared to remain stable in time after therapy (Fig 4B). As a consequence, LVEF seemed slightly decreased in CPC treated mice (-3.9 ± 2.7%) compared to a minor increase (+1,26 ± 1.8%) in vehicle control (p = 0.16; Fig 4C).

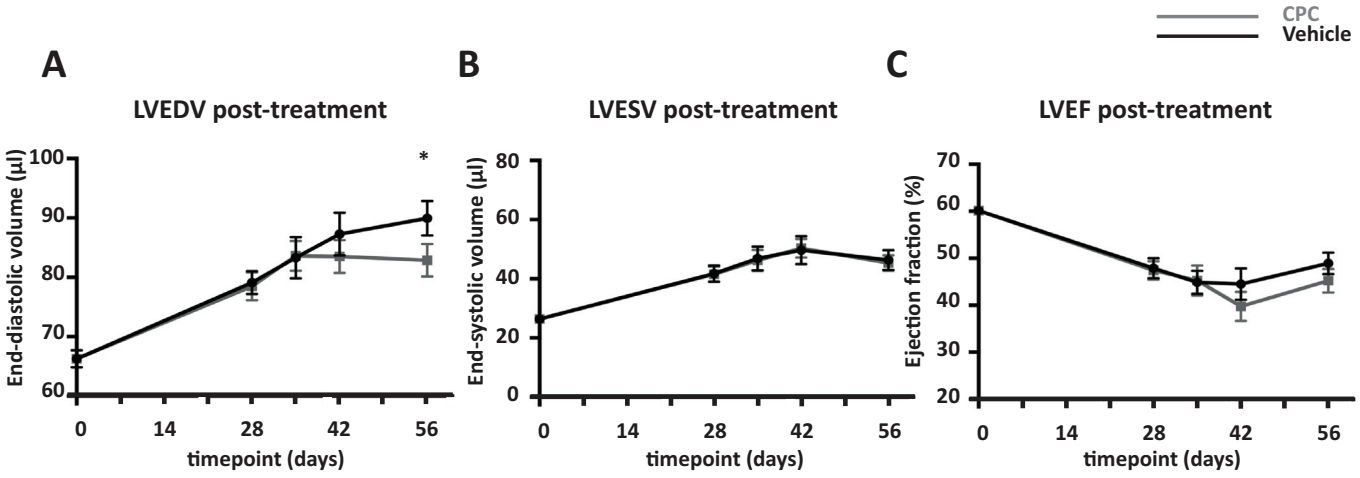

Fig 4. Functional outcome measurements by echocardiography at 1 month follow-up demonstrated preservation of the end-diastolic volume. A) LVEDV in the CPC group differed from the control group at experimental day 56 (post-treatment). No significant difference between the groups was observed for (**B**) LVESV and (**C**) LVEF. Black lines indicate vehicle treated mice (n = 16) and grey lines indicate mice treated with CPC (n = 13). * p< 0.05.

https://doi.org/10.1371/journal.pone.0173657.g004

Matrix composition 28 days after CPC treatment

Since CPC solely affected the LVEDV we sought to identify local effects of CPC on the infarcted tissue and extracellular matrix. The infarct size, defined as the percentage of non-viable left ventricle, was slightly lower in the CPC group (8.0 ± 2.5% vs. 10.6 ± 1.8%, p = ns). Accordingly, mice treated with CPC seemed to have a lower collagen density compared to vehicle-treated mice (4.6 ± 0.46 vs. 5.0 ± 0.54, mean grey value per mm^2 infarct area, p = ns, Fig 5A and 5B). Further analysis of the composition of the extracellular matrix showed that although both groups had similar amounts of matrix producing cells ($vimentin^+$ cells) in the infarcted area, the ratio of collagen type I/III appeared higher in mice treated with CPC (Fig 5A and 5D). All effects in matrix composition favored the CPC group, not reaching statistical significance (Fig 5E).

To determine if CPC increased the vascularization of the infarct area, like we demonstrated before in an acute injury model [21], a staining for CD31 and alpha smooth muscle actin (α-SMA) positive vessels was performed (Fig 5F). The staining demonstrated a higher vascular density in the infarcted area compared to the remote area (22.1 ± 1.7 vs. 12.1 ± 1.6, vessels/ mm^2, $p < 0.001$). Treatment with CPC did not result in an increased vascularization (20.8 ± 2.2 vessels/mm^2) in the infarct area compared to vehicle treatment (23.3± 2.6 vessels/ mm^2). In addition, no difference in $CD45^+$ cells (granulocytes) was observed between the groups in the infarcted area.

Speckle tracking analysis is sensitive for early changes in matrix composition

As our histological data demonstrated, no significant difference could be observed for the analyzed individual parameters between CPC or vehicle treated mice. In order to clarify the observed attenuation of the LVEDV, we used speckle tracking analysis for more detailed visualization of the regional wall motion dimensions of the myocardium (Fig 6A–6E). Upon I/R injury an expected decline in velocity, strain and SR was observed (Table 1). Global radial deformation changes were more pronounced than longitudinal deformation changes (S1 Table), with the latter being more affected in the infarcted region. Although no differences between the groups were found in conventional cardiac parameters (LVEDV and LVESV) prior to treatment, small differences were observed between the CPC group and vehicle group for radial velocity and SR, with a better performance for the vehicle group. Radial velocity was 0.7 ± 0.06 cm/s in the CPC group and 0.9 ± 0.06 cm/s in the vehicle group (p = 0.02). SR was 6.1 ± 0.4%/s in the CPC group vs. 8.0 ± 0.6%/s in the vehicle group (p = 0.01; Table 1).

To gain insight in the effect of treatment, the difference of post- and pre-treatment was calculated for all individual mice (Table 1). None of the longitudinal measurements were different between the two groups. However, analysis of myocardial deformation on the radial axis did show significant differences over time in favor of the CPC group. Radial velocity was increased in CPC treated mice (+0.2 ± 0.1 cm/s) while further decreased in vehicle treated mice (-0.1 ± 0.06 cm/s, p = 0.02). Likewise, strain and SR significantly improved for CPC treatment compared to vehicle. SR improved from 6.1 ± 0.4/s to 7.1 ± 0.6/s compared to a decrease (8.0 ± 0.6/s to 7.3 ± 0.6/s) for vehicle treatment.

Discussion

Recently provided recommendations by the European Society of Cardiology, Working Group Cellular Biology of the Heart [20], aim to improve the therapeutic application of cell-based therapies for cardiac regeneration and repair by, among other recommendations, using more appropriate animal models that better resemble human chronic ischemic disease.

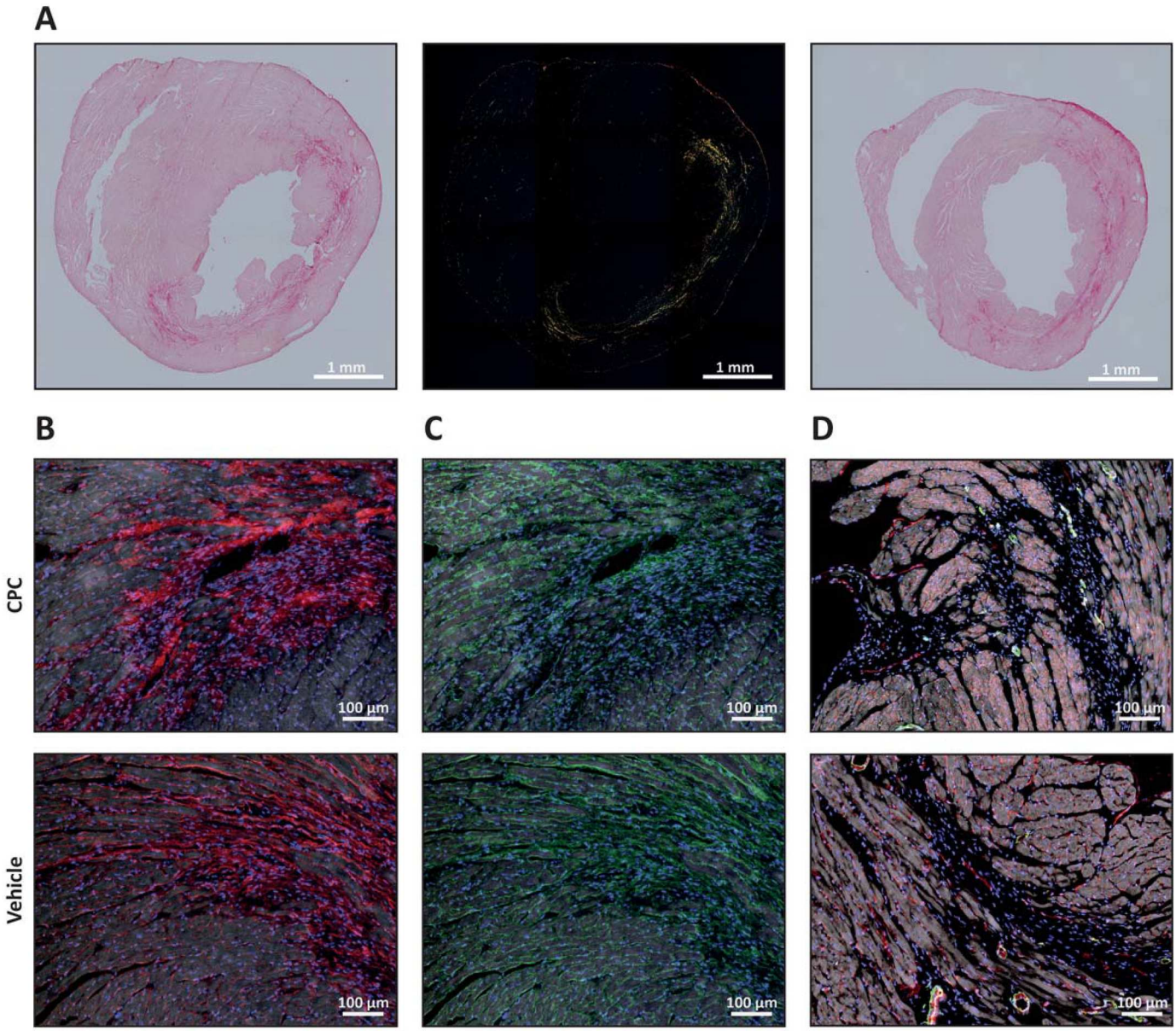

E

	CPC		Vehicle		p-value
	Infarct	*Remote*	*Infarct*	*Remote*	
Infarct size (%)	8.0 ± 2.5	-	10.6 ± 1.8	-	ns
Picrosirius (mean grey value)	4.6 ± 0.5	-	5.0 ± 0.5	-	ns
Vimentin (+ area/infarct)	6.5 ± 0.7	-	6.7 ± 1.8	-	ns
Col I (+ area/infarct)	30.0 ± 6.3	22.3 ± 4.0	34.4 ± 6.4	21.5 ± 3.6	ns
Col III (+ area/infarct)	28.4 ± 4.7	24.4 + 4.6	36.3 ± 6.4	32.8 ± 5.0	ns
Col I/III (ratio)	1.08 ± 0.13	0.67 ± 0.10	0.79 ± 0.13	0.55 ± 0.13	ns
vessels (CD31+,α-SMA+/area)	20.8 ± 2.2	11.1 ± 2.7	23.3 ± 2.6	12.9 ± 1.8	ns
granylocytes (CD45+/area)	1.9 ± 0.3	1.1 ± 0.3	1.5 ± 0.2	1.6 ± 0.4	ns

Fig 5. Histological analysis of matrix composition in the injured myocardium. Representative images of cryosections stained with picrosirius red used for quantification of the collagen density of the infarcted area (**A**). The left and middle panels show a brightfield and polarized light image of the

CPC group, repectively. The right image represents the vehicle treated group. The collagen composition was assessed by immunofluorescent imaging of (**B**) collagen type I (red) and (**C**) collagen type III (green). (**D**) Immunofluorescent staining showed an increase of $CD31^+$ (red) and a-SMA^+ (green) vessels in the infarcted area compared to the remote area. No difference was observed between CPC or vehicle treated mice. Nuclei were stained with Hoechst (blue) and the myocardial structure is shown in grey. In **B-D** the upper panel represents the CPC group and the lower panel the vehicle group. (**E**) Table with quantification of the stainings.

https://doi.org/10.1371/journal.pone.0173657.g005

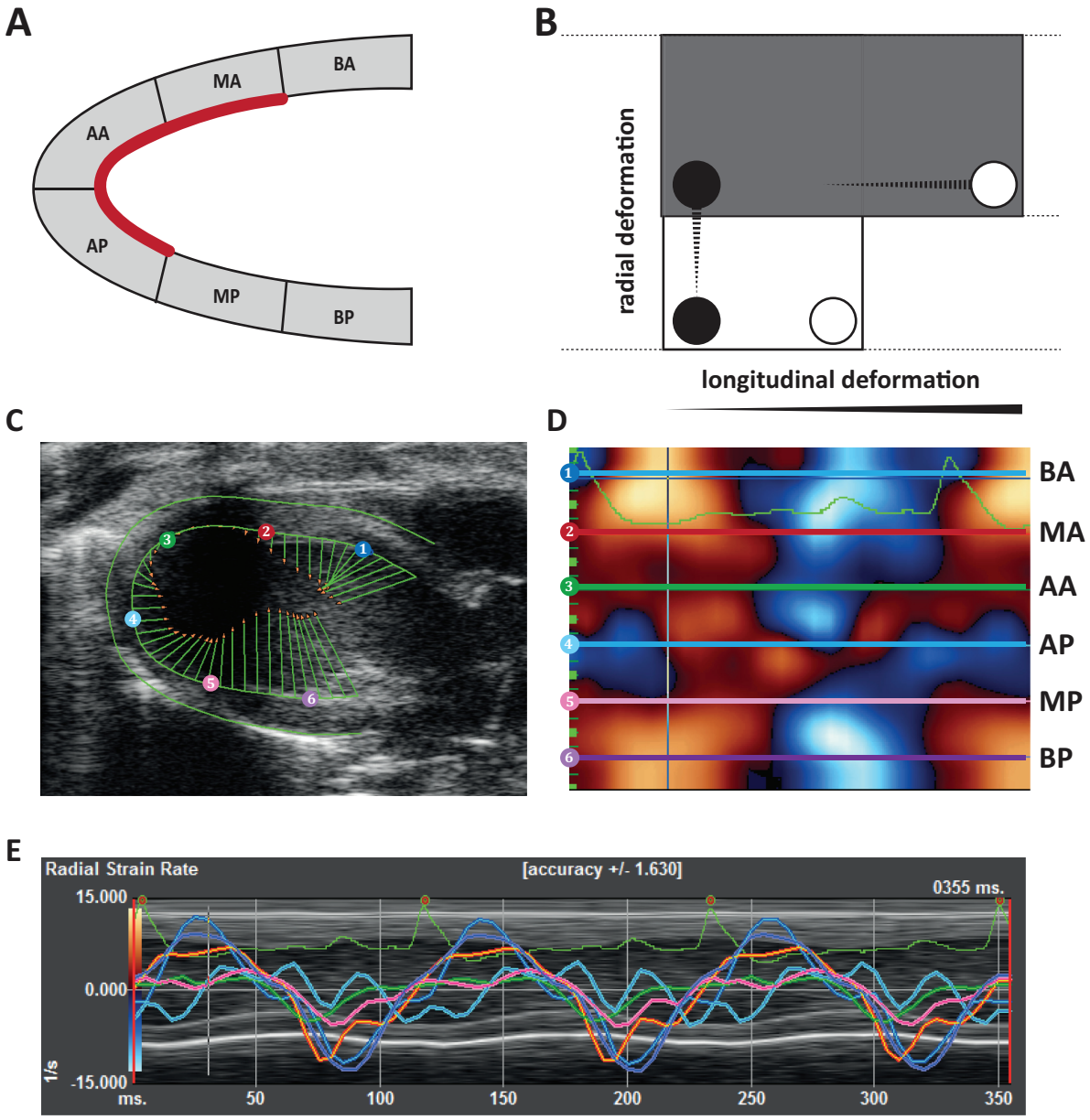

Fig 6. Myocardial deformation. (**A**) Schematic overview of 6 myocardial segments and deformation vectors; Basal-anterior (BA), mid-anterior (MA), apical-anterior (AA), apical-posterior (AP), mid-posterior (MP), basal-posterior (BP). Red line indicates infarct region. (**B**) Graphic representation of radial and longitudinal deformation. (**C**) Representative echocardiographic image of myocardial deformation (radial SR) after I/R injury, with concomitant vector lines, (**D**) for individual tracking points, and (**E**) combined with electrocardiogram and short axis view.

https://doi.org/10.1371/journal.pone.0173657.g006

Table 1. Regional myocardial deformation. Segments denoted as infarct area (MA, AA, AP) were used for quantification of velocity, strain and SR. The average value of the infarct area is given for the deformation parameters (velocity, strain and SR). p-values in the baseline column denote differences between baseline and 28 days I/R. In addition, p-values in the pre-treatment and post-treatment column show differences between the CPC and vehicle group.

Regional deformation	baseline		pre-treatment				post-treatment (delta)		
	overall		overall (n = 29)	CPC (n = 13)	Vehicle (n = 16)		CPC (n = 13)	Vehicle (n = 16)	
Radial									
velocity (cm/s)	1.1±0.08	**0.0002**	0.8±0.04	0.7±0.06	0.9±0.06	**0.0193**	0.1±0.04	-0.1±0.06	**0.0056**
strain (%)	35.4±3.3	**0.0007**	21.6±2.0	18.8±2.3	23.9±3.2	0.218	4.7±2.1	-1.2±3.1	0.1548
SR (1/s)	9.8±0.4	**0.0003**	7.2±0.4	6.1±0.4	8.0±0.6	**0.0131**	1.0±0.5	-0.7±0.6	**0.0409**
Longitudinal									
velocity (cm/s)	0.9±0.07	0.0829	0.7±0.05	0.7±0.1	0.7±0.05	0.6916	0.06±0.1	0.04±0.1	0.8709
strain (%)	-17.9±1.9	**0.0039**	-12.8±0.7	-12.1±0.9	-13.4±11	0.3713	-0.8±1.0	-0.08±1.1	0.6614
SR (1/s)	-7.2±0.6	**0.0046**	-5.3±0.3	-5.0±0.5	-5.5±0.5	0.4912	0.2±0.3	0.1±0.5	0.5984

https://doi.org/10.1371/journal.pone.0173657.t001

According to this, we tested CPC therapy in a clinically relevant mouse model of chronic cardiac remodeling. Minimally invasive intramyocardial injection of CPC was successfully applied 28 days after I/R injury and resulted in localized long-term engraftment. Although limited, transplantation of CPC resulted in attenuation of left ventricular dilatation and improved regional SR at 4 weeks follow-up with an effect size more closely resembling the results as obtained in large animal models and clinical studies. The challenge of clinical translation of cell therapy in small animal models is anticipated in this study by using an appropriate chronic I/R injury model with minimally invasive local therapy and clinically applicable functional outcome parameters.

We started off with a systematic assessment of the effect of CPC in sub-acute and chronic MI models compared to the acute setting. Our analyses show a large spread in effect size of CPC applied in the chronic setting and display a clear discrepancy in the number of small animal studies in chronic cardiac remodeling as compared to acute MI, which is worrisome due to the need for translation of this therapy to heart failure patients in particular. The observed translational failure in effect size might be attributed to animal size, but could also be caused by the models used, since 5 out of 11 placebo-controlled large animal CPC studies were done in chronic MI models, compared to only 2 out of 95 studies in small animal models [9].

Both Tang *et al*. and Tseliou *et al*. demonstrated an improvement of the LVEF upon treatment with CPC in a rat model of chronic cardiac injury with application of CPC 4 weeks after ischemic injury [14, 15]. Likewise, it was demonstrated that CPC treatment applied 7 days after permanent ligation of the LAD in mice resulted in improvement of LVEF and a lowering of the ventricular scar burden [17]. In contrast to these results, we found that the application of CPC in a murine chronic I/R model did not result in significant restoration of cardiac function. However, it is noteworthy that our results demonstrated an early preservation of the diastolic diameter of the left ventricle upon CPC injection.

The apparent discrepancy in treatment effects between performed studies, including ours, is most likely attributed to the timing of therapy, the used injury model, delivery method, source of CPC and cell retention. Our study was designed to mimic the human clinical situation of chronic ischemic heart failure with timing of therapy as a key prerequisite. Accordingly, we used a model of I/R injury to provide insight in the effect of human CPC in negative remodeling. To prevent immune reaction we used immune deficient (NOD-SCID) mice to accomplish that goal. Although a recent published report demonstrated that I/R injury in NOD-SCID mice does not result in sufficient cardiac damage [28], we show successful induction of cardiac remodeling upon I/R injury. Moreover, we administered local therapy 4 weeks

after induction of MI to predominantly target chronic cardiac remodeling. In contrast, the previously described treatment at 7 days interferes with the extinguishing acute inflammatory response [29]. It is important to note that the therapeutic effect of cell therapy will be different in the distinct phases of cardiac injury and repair, e.g. tissue salvage in the acute phase and tissue remodeling in the chronic phase [12].

In line with the small beneficial results obtained in pre-clinical large animal research and clinical trials [30, 31], we demonstrated an attenuation of LVEDV increase upon treatment with CPC. In addition, there seems to be a difference in therapeutic benefit in mice with respect to pre-treatment extent of injury. These findings are in accordance with clinical meta-analysis demonstrating more effective treatment in patients with more severe cardiac dysfunction at the start of the therapy [32, 33].

With only two other placebo-controlled CPC studies in small animal models, the difference in beneficial effects remains difficult to explain and timing of therapy needs further exploration to better understand the role of the chosen injury model. In addition, it is known that CPC isolated with different isolation protocols display slightly dissimilar markers. However, this difference most likely did not influence the treatment effect since a high degree of similarity is found in their individual transcriptomes, although Cardiospheres displayed a higher secretory pattern of molecules involved in the development of cardiac muscle, vasculogenesis and angiogenesis [34].

Since we observed an effect of CPC treatment on eccentric cardiac remodeling, we assessed histological parameters to provide insight in the structural and cellular changes of the myocardial matrix. Although infarct size and collagen density appeared slightly smaller in the treated group, a direct link between histological parameters and the observed changes in cardiac volumes were absent. Since histological assessment is subject to a need for sample selection and thereby creates additional experimental variation or bias, the findings do not rule out that CPC interferes with matrix remodeling. Recently, it was demonstrated that CPC reduced fibroblast proliferation and attenuated pro-fibrotic signaling in a rat model of chronic MI [35]. This notion is supported by the observed long term improved left ventricular remodeling upon CPC treatment [14, 15, 36]. Several reports suggest that early changes in matrix remodeling are detected with a higher sensitivity with measurements of regional wall motion parameters by speckle tracking analysis [37–40]. Therefore, we assessed velocity, strain and SR of the infarcted region and indeed we have identified beneficial regional deformation changes upon CPC treatment, consistent with another study showing improved strain and SR upon myocardial treatment with induced pluripotent stem cells [41].

Implementation of regional wall motion measurements in small animal research might be valuable to identify more sensitive markers of cardiac function and cardiac improvement upon novel therapies. In parallel, these novel techniques merit further investigation to identify key modulators of myocardial remodeling translatable to pre-clinical large animal models and clinical cell therapy studies.

The resemblance of effect size with (pre-)clinical studies in literature underlines the translatability of our small animal injury model and shows that the apparent discrepancy in results can possibly be explained by the various approaches in the different models, of which timing of therapy and the type of injury model used are presumably the most important factors.

The model we present here can be exerted as a starting point to study the basic mechanisms behind cell therapy and to introduce more advanced methods in small animal research to examine therapies already tested in the acute post-MI phase. The tentative positive outcome of cell therapy in (pre-)clinical trials and the limited observed effects in our study force us to take the long view and to carefully address opportunities to optimize cell therapy to achieve clinical

efficacy. Recently, tissue engineering approaches with the use of cell carriers improved initial cell retention and consequently resulted in a more beneficial treatment effect [42–44]. Furthermore, tailoring of cell differentiation protocols to direct cell faith is another promising approach to enhance therapeutic potential [45]. Therefore, exploration of different biomaterials and enhancing cell effectors would be of interest in future studies. To further maximize the success of preclinical research, a shift towards humanized small animal models should be made. By integrating aspects of the human immune system into mice models, a more comparable pathophysiology is created to study the multicellular interplay of cardiac remodeling upon I/R injury. Besides, co-morbidities and pharmacological agents should be incorporated in preclinical animal models [46–48]. The add-on effect of stem cell therapy will become clear when applied in combination with factors as hypercholesterolemia, diabetes, age, renal failure and gender [49].

Driven by the urge for clinical translation through proper animal models [50], the present study demonstrates a comprehensive small animal injury model to study chronic cardiac remodeling. We found that CPC transplantation can be adequately examined in this study set-up and by that provide a translatable small animal model facilitating advances in research for new local therapeutic approaches to treat chronic heart failure.

Supporting information

S1 Appendix. Supplementary methods.
(DOCX)

S1 Fig. Meta-regression of timing of CPC therapy in small animal models. Analysis of CPC studies in small animal models showed a large spread in effect on EF for timing of therapy ($p = 0.26$) with only 2 studies performed in the chronic MI setting.
(EPS)

S2 Fig. Reconstructed 3D echocardiography. (A) Representative images of the contours of the LVEDV and (B) LVESV in a reconstructed 3D echocardiographic image. Bottom panels show examples of the contours drawn in the short axis images used to reconstruct the left ventricle.
(TIFF)

S3 Fig. Subgroup analysis of functional outcome. (**A**) LVEDV is not preserved in mice with low retention at day 2 (unsuccessful injection). Black line indicates vehicle treated mice, grey line indicates mice with successful CPC injection and dotted grey line indicates mice with unsuccessful CPC injection. LVEDV = left ventricular end-diastolic volume. (**B**) The effect of treatment is higher in mice with a larger injury extent. Groups are divided by the median LVEDV as measured prior to treatment. * $p < 0.05$.
(EPS)

S1 Table. Global myocardial deformation. All 6 myocardial segments were used for quantification of velocity, strain and SR. p-values in the baseline column denote differences between baseline and 28 days I/R. In addition, p-values in the pre-treatment and post-treatment column show differences between the CPC and vehicle group.
(DOCX)

Acknowledgments

We would like to acknowledge H. Gremmels for the lamin A/C antibody.

Author Contributions

Conceptualization: JCD PPZ DAF MAB SS LWvL JPS PAD.

Data curation: JCD PPZ DAF MAB SS.

Formal analysis: JCD PPZ DAF MAB.

Funding acquisition: JPS PAD.

Investigation: JCD PPZ DAF MAB SS.

Methodology: JCD PPZ DAF MAB JPS.

Project administration: JCD MAB.

Resources: MAB DAF.

Supervision: DAF SS LWvL JPS PAD.

Validation: JCD.

Visualization: JCD PPZ.

Writing – original draft: JCD PPZ.

Writing – review & editing: JCD PPZ DAF MAB SS LWvL JPS PAD.

References

1. Lecour S, Bøtker HE, Condorelli G, Davidson SM, Garcia-Dorado D, Engel FB, et al. ESC working group cellular biology of the heart: position paper: improving the preclinical assessment of novel cardioprotective therapies. Cardiovasc Res 2014; 104:399–411. https://doi.org/10.1093/cvr/cvu225 PMID: 25344369
2. Mozaffarian D, Benjamin EJ, Go AS, Arnett DK, Blaha MJ, Cushman M, et al. Heart Disease and Stroke Statistics-2016 Update: A Report From the American Heart Association. Circulation 2015; 133:e38–e360. https://doi.org/10.1161/CIR.0000000000000350 PMID: 26673558
3. Menasché P, Hagège AA, Scorsin M, Pouzet B, Desnos M, Duboc D, et al. Myoblast transplantation for heart failure. Lancet (London, England) 2001; 357:279–80.
4. Strauer BE, Brehm M, Zeus T, Köstering M, Hernandez A, Sorg R V, et al. Repair of infarcted myocardium by autologous intracoronary mononuclear bone marrow cell transplantation in humans. Circulation 2002; 106:1913–8. PMID: 12370212
5. Abdel-Latif A, Bolli R, Tleyjeh IM, Montori VM, Perin EC, Hornung CA, et al. Adult bone marrow-derived cells for cardiac repair: a systematic review and meta-analysis. Arch Intern Med 2007; 167:989–97. https://doi.org/10.1001/archinte.167.10.989 PMID: 17533201
6. Schächinger V, Erbs S, Elsässer A, Haberbosch W, Hambrecht R, Hölschermann H, et al. Intracoronary bone marrow-derived progenitor cells in acute myocardial infarction. N Engl J Med 2006; 355:1210–21. https://doi.org/10.1056/NEJMoa060186 PMID: 16990384
7. Makkar RR, Smith RR, Cheng K, Malliaras K, Thomson LEJ, Berman D, et al. Intracoronary cardiosphere-derived cells for heart regeneration after myocardial infarction (CADUCEUS): a prospective, randomised phase 1 trial. Lancet (London, England) 2012; 379:895–904.
8. Lara-Pezzi E, Menasché P, Trouvin J-H, Badimón L, Ioannidis JPA, Wu JC, et al. Guidelines for translational research in heart failure. J Cardiovasc Transl Res 2015; 8:3–22. https://doi.org/10.1007/s12265-015-9606-8 PMID: 25604959
9. Zwetsloot PP, Végh AM, Jansen Of Lorkeers SJ, van Hout GP, Currie GL, Sena ES, et al. Cardiac Stem Cell Treatment in Myocardial Infarction: A Systematic Review and Meta-Analysis of Preclinical Studies. Circ Res 2016.
10. Jansen Of Lorkeers SJ, Eding JEC, Vesterinen HM, van der Spoel TIG, Sena ES, Duckers HJ, et al. Similar effect of autologous and allogeneic cell therapy for ischemic heart disease: systematic review and meta-analysis of large animal studies. Circ Res 2015; 116:80–6. https://doi.org/10.1161/CIRCRESAHA.116.304872 PMID: 25186794

11. Tongers J, Losordo DW, Landmesser U. Stem and progenitor cell-based therapy in ischaemic heart disease: promise, uncertainties, and challenges. Eur Heart J 2011; 32:1197–206. https://doi.org/10.1093/eurheartj/ehr018 PMID: 21362705

12. Goumans M-J, Maring JA, Smits AM. A straightforward guide to the basic science behind cardiovascular cell-based therapies. Heart 2014; 100:1153–7. https://doi.org/10.1136/heartjnl-2014-305646 PMID: 24993501

13. Oskouei BN, Lamirault G, Joseph C, Treuer A V, Landa S, Da Silva J, et al. Increased potency of cardiac stem cells compared with bone marrow mesenchymal stem cells in cardiac repair. Stem Cells Transl Med 2012; 1:116–24. https://doi.org/10.5966/sctm.2011-0015 PMID: 23197758

14. Tseliou E, Reich H, de Couto G, Terrovitis J, Sun B, Liu W, et al. Cardiospheres reverse adverse remodeling in chronic rat myocardial infarction: roles of soluble endoglin and Tgf-β signaling. Basic Res Cardiol 2014; 109:443. https://doi.org/10.1007/s00395-014-0443-8 PMID: 25245471

15. Tang X-L, Rokosh G, Sanganalmath SK, Yuan F, Sato H, Mu J, et al. Intracoronary administration of cardiac progenitor cells alleviates left ventricular dysfunction in rats with a 30-day-old infarction. Circulation 2010; 121:293–305. https://doi.org/10.1161/CIRCULATIONAHA.109.871905 PMID: 20048209

16. Rota M, Padin-Iruegas ME, Misao Y, De Angelis A, Maestroni S, Ferreira-Martins J, et al. Local activation or implantation of cardiac progenitor cells rescues scarred infarcted myocardium improving cardiac function. Circ Res 2008; 103:107–16. https://doi.org/10.1161/CIRCRESAHA.108.178525 PMID: 18556576

17. Latham N, Ye B, Jackson R, Lam B-K, Kuraitis D, Ruel M, et al. Human blood and cardiac stem cells synergize to enhance cardiac repair when cotransplanted into ischemic myocardium. Circulation 2013; 128:S105–12. https://doi.org/10.1161/CIRCULATIONAHA.112.000374 PMID: 24030393

18. Springer ML, Sievers RE, Viswanathan MN, Yee MS, Foster E, Grossman W, et al. Closed-chest cell injections into mouse myocardium guided by high-resolution echocardiography. Am J Physiol Heart Circ Physiol 2005; 289:H1307–14. https://doi.org/10.1152/ajpheart.00164.2005 PMID: 15908468

19. Prendiville TW, Ma Q, Lin Z, Zhou P, He A, Pu WT. Ultrasound-guided transthoracic intramyocardial injection in mice. J Vis Exp 2014:e51566. https://doi.org/10.3791/51566 PMID: 25146757

20. Madonna R, Van Laake LW, Davidson SM, Engel FB, Hausenloy DJ, Lecour S, et al. Position Paper of the European Society of Cardiology Working Group Cellular Biology of the Heart: cell-based therapies for myocardial repair and regeneration in ischemic heart disease and heart failure. Eur Heart J 2016.

21. Smits AM, van Laake LW, den Ouden K, Schreurs C, Szuhai K, van Echteld CJ, et al. Human cardiomyocyte progenitor cell transplantation preserves long-term function of the infarcted mouse myocardium. Cardiovasc Res 2009; 83:527–35. https://doi.org/10.1093/cvr/cvp146 PMID: 19429921

22. Smits AM, van Vliet P, Metz CH, Korfage T, Sluijter JP, Doevendans P a, et al. Human cardiomyocyte progenitor cells differentiate into functional mature cardiomyocytes: an in vitro model for studying human cardiac physiology and pathophysiology. Nat Protoc 2009; 4:232–243. https://doi.org/10.1038/nprot.2008.229 PMID: 19197267

23. Goumans M-J, de Boer TP, Smits AM, van Laake LW, van Vliet P, Metz CHG, et al. TGF-beta1 induces efficient differentiation of human cardiomyocyte progenitor cells into functional cardiomyocytes in vitro. Stem Cell Res 2007; 1:138–149. https://doi.org/10.1016/j.scr.2008.02.003 PMID: 19383394

24. Feyen D, Gaetani R, Liu J, Noort W, Martens A, den Ouden K, et al. Increasing short-term cardiomyocyte progenitor cell (CMPC) survival by necrostatin-1 did not further preserve cardiac function. Cardiovasc Res 2013; 99:83–91. https://doi.org/10.1093/cvr/cvt078 PMID: 23554461

25. van Laake LW, Passier R, Monshouwer-Kloots J, Nederhoff MG, Ward-van Oostwaard D, Field LJ, et al. Monitoring of cell therapy and assessment of cardiac function using magnetic resonance imaging in a mouse model of myocardial infarction. Nat Protoc 2007; 2:2551–67. https://doi.org/10.1038/nprot.2007.371 PMID: 17947998

26. Xu Z, Alloush J, Beck E, Weisleder N. A murine model of myocardial ischemia-reperfusion injury through ligation of the left anterior descending artery. J Vis Exp 2014.

27. Motulsky HJ, Brown RE. Detecting outliers when fitting data with nonlinear regression—a new method based on robust nonlinear regression and the false discovery rate. BMC Bioinformatics 2006; 7:123. https://doi.org/10.1186/1471-2105-7-123 PMID: 16526949

28. van Zuylen V-L, den Haan MC, Roelofs H, Fibbe WE, Schalij MJ, Atsma DE. Myocardial infarction models in NOD/Scid mice for cell therapy research: permanent ischemia vs ischemia-reperfusion. Springerplus 2015; 4:336. https://doi.org/10.1186/s40064-015-1128-y PMID: 26185738

29. van den Akker F, Deddens JC, Doevendans PA, Sluijter JPG. Cardiac stem cell therapy to modulate inflammation upon myocardial infarction. Biochim Biophys Acta 2013; 1830:2449–58. https://doi.org/10.1016/j.bbagen.2012.08.026 PMID: 22975401

30. Johnston P V, Sasano T, Mills K, Evers R, Lee S-T, Smith RR, et al. Engraftment, differentiation, and functional benefits of autologous cardiosphere-derived cells in porcine ischemic cardiomyopathy. Circulation 2009; 120:1075–83, 7 p following 1083. https://doi.org/10.1161/CIRCULATIONAHA.108.816058 PMID: 19738142

31. Jansen Of Lorkeers SJ, Gho JMIH, Koudstaal S, van Hout GPJ, Zwetsloot PPM, van Oorschot JWM, et al. Xenotransplantation of Human Cardiomyocyte Progenitor Cells Does Not Improve Cardiac Function in a Porcine Model of Chronic Ischemic Heart Failure. Results from a Randomized, Blinded, Placebo Controlled Trial. PLoS One 2015; 10:e0143953. https://doi.org/10.1371/journal.pone.0143953 PMID: 26678993

32. Delewi R, Hirsch A, Tijssen JG, Schächinger V, Wojakowski W, Roncalli J, et al. Impact of intracoronary bone marrow cell therapy on left ventricular function in the setting of ST-segment elevation myocardial infarction: a collaborative meta-analysis. Eur Heart J 2014; 35:989–98. https://doi.org/10.1093/eurheartj/eht372 PMID: 24026778

33. Clifford DM, Fisher SA, Brunskill SJ, Doree C, Mathur A, Clarke MJ, et al. Long-term effects of autologous bone marrow stem cell treatment in acute myocardial infarction: factors that may influence outcomes. PLoS One 2012; 7:e37373. https://doi.org/10.1371/journal.pone.0037373 PMID: 22655042

34. Gaetani R, Feyen DAM, Doevendans PA, Gremmels H, Forte E, Fledderus JO, et al. Different types of cultured human adult cardiac progenitor cells have a high degree of transcriptome similarity. J Cell Mol Med 2014; 18:2147–51. https://doi.org/10.1111/jcmm.12458 PMID: 25311343

35. Yee K, Malliaras K, Kanazawa H, Tseliou E, Cheng K, Luthringer DJ, et al. Allogeneic cardiospheres delivered via percutaneous transendocardial injection increase viable myocardium, decrease scar size, and attenuate cardiac dilatation in porcine ischemic cardiomyopathy. PLoS One 2014; 9:e113805. https://doi.org/10.1371/journal.pone.0113805 PMID: 25460005

36. Tang X-L, Li Q, Rokosh G, Sanganalmath S, Chen N, Ou Q, et al. Long-Term Outcome of Administration of c-kitPOS Cardiac Progenitor Cells After Acute Myocardial Infarction: Transplanted Cells Do Not Become Cardiomyocytes, but Structural and Functional Improvement and Proliferation of Endogenous Cells Persist for At Lea. Circ Res 2016.

37. Thibault H, Gomez L, Donal E, Pontier G, Scherrer-Crosbie M, Ovize M, et al. Acute myocardial infarction in mice: assessment of transmurality by strain rate imaging. Am J Physiol Heart Circ Physiol 2007; 293:H496–502. https://doi.org/10.1152/ajpheart.00087.2007 PMID: 17384134

38. Bauer M, Cheng S, Jain M, Ngoy S, Theodoropoulos C, Trujillo A, et al. Echocardiographic speckle-tracking based strain imaging for rapid cardiovascular phenotyping in mice. Circ Res 2011; 108:908–16. https://doi.org/10.1161/CIRCRESAHA.110.239574 PMID: 21372284

39. Peng Y, Popovic ZB, Sopko N, Drinko J, Zhang Z, Thomas JD, et al. Speckle tracking echocardiography in the assessment of mouse models of cardiac dysfunction. Am J Physiol Heart Circ Physiol 2009; 297:H811–20. https://doi.org/10.1152/ajpheart.00385.2009 PMID: 19561310

40. Bhan A, Sirker A, Zhang J, Protti A, Catibog N, Driver W, et al. High-frequency speckle tracking echocardiography in the assessment of left ventricular function and remodeling after murine myocardial infarction. Am J Physiol Heart Circ Physiol 2014; 306:H1371–83. https://doi.org/10.1152/ajpheart.00553.2013 PMID: 24531814

41. Yamada S, Nelson TJ, Kane GC, Martinez-Fernandez A, Crespo-Diaz RJ, Ikeda Y, et al. Induced pluripotent stem cell intervention rescues ventricular wall motion disparity, achieving biological cardiac resynchronization post-infarction. J Physiol 2013; 591:4335–49. https://doi.org/10.1113/jphysiol.2013.252288 PMID: 23568891

42. Feyen DAM, Gaetani R, Deddens J, van Keulen D, van Opbergen C, Poldervaart M, et al. Gelatin Microspheres as Vehicle for Cardiac Progenitor Cells Delivery to the Myocardium. Adv Healthc Mater 2016.

43. van den Akker F, Feyen DAM, van den Hoogen P, van Laake LW, van Eeuwijk ECM, Hoefer I, et al. Intramyocardial stem cell injection: go(ne) with the flow. Eur Heart J 2016.

44. Ye Z, Zhou Y, Cai H, Tan W. Myocardial regeneration: Roles of stem cells and hydrogels. Adv Drug Deliv Rev 2011; 63:688–97. https://doi.org/10.1016/j.addr.2011.02.007 PMID: 21371512

45. Aguirre A, Sancho-Martinez I, Izpisua Belmonte JC. Reprogramming toward heart regeneration: stem cells and beyond. Cell Stem Cell 2013; 12:275–84. https://doi.org/10.1016/j.stem.2013.02.008 PMID: 23472869

46. McMurray JJ V, Adamopoulos S, Anker SD, Auricchio A, Böhm M, Dickstein K, et al. ESC guidelines for the diagnosis and treatment of acute and chronic heart failure 2012: The Task Force for the Diagnosis and Treatment of Acute and Chronic Heart Failure 2012 of the European Society of Cardiology. Developed in collaboration with the Heart. Eur J Heart Fail 2012; 14:803–69.

47. Giricz Z, Lalu MM, Csonka C, Bencsik P, Schulz R, Ferdinandy P. Hyperlipidemia attenuates the infarct size-limiting effect of ischemic preconditioning: role of matrix metalloproteinase-2 inhibition. J Pharmacol Exp Ther 2006; 316:154–61. https://doi.org/10.1124/jpet.105.091140 PMID: 16166272

48. Baranyai T, Nagy CT, Koncsos G, Onódi Z, Károlyi-Szabó M, Makkos A, et al. Acute hyperglycemia abolishes cardioprotection by remote ischemic perconditioning. Cardiovasc Diabetol 2015; 14:151. https://doi.org/10.1186/s12933-015-0313-1 PMID: 26581389

49. McCafferty K, Forbes S, Thiemermann C, Yaqoob MM. The challenge of translating ischemic conditioning from animal models to humans: the role of comorbidities. Dis Model Mech 2014; 7:1321–33. https://doi.org/10.1242/dmm.016741 PMID: 25481012

50. Bolli R, Ghafghazi S. Cell Therapy Needs Rigorous Translational Studies in Large Animal Models. J Am Coll Cardiol 2015; 66:2000–4. https://doi.org/10.1016/j.jacc.2015.09.002 PMID: 26516003